[Article ID] 1003 - 6326(2000)04 - 0524 - 07

Electric arc furnace dust non-isothermal reduction kinetics①

ZHANG Chuan-fu(张传福)[1], PENG Bing(彭 兵)[1], PENG Ji(彭 及)[1],
J. Lobel[2], A. K. Janusz[2]
(1. Department of Metallurgical Science and Engineering,
Central-South University of Technology, Changsha 410083, P.R.China;
2. The Department of Metallurgical Engineering,
McGill University, Montreal, QC, H3A 2B2, Canada)

[Abstract] Kinetic studies of the electric arc furnace (EAF) dust reduction process have been carried out under non-isothermal temperature condition. EAF dust pellets were made with carbon as the reducing agent and dolomite as the binder. A Thermo-Gravimetric Analyzer (TGA) was used to determine the mass loss of pellets, which were heated at an average rate of 40 K/min up to 1 500 ℃. The reduction degree was calculated by consideration of the pellet mass loss, evaporation of moisture, dust, zinc and lead at high temperature. The reduction process of EAF dust was divided into three steps related to the change in temperature and time. The non-isothermal reduction kinetics equations were set up to describe every step. The kinetics parameters such as apparent activation energies and frequency factors were established at the same time. It was found that the first step is chemically controlled, the second step is diffusion-controlled and the third step is strongly dependent on the initial content of carbon in the pellet. CrO can be reduced only in the last step by high temperature and high initial carbon content.

[Key words] EAF dust recycles; chemical kinetics; non-isothermal reduction
[CLC number] TF741.5 [Document code] A

1 INTRODUCTION

The airborne fine particulate Electric Arc Furnace (EAF) dust is generated in the steel manufacturing process when scrap is electrically melted. It is considered as a hazardous waste because of leaching characteristic of heavy metals such as lead, zinc and chromium, which are present in the EAF dust. Thus, it is not permitted to dispose the EAF dust in conventional landfills. There are many recycling methods developed for the dust[1~7], but most of them are not commercially available. One of the economical ways seems to be a direct recovery of the metals from the dust during the steelmaking process. It is a self-reduction and self-recycling process, in which EAF dust and reducing agent is mixed well, pellets are maken with the binder, the pellets are added to the electric arc furnace during steelmaking. The oxidized metals in the dust can be reduced by the reducing agent and recovered to the steel. Especially in the stainless steelmaking, there are a lot of valuable metal elements such as nickel and chromium in the dust. They can be recycled to the stainless steel in this way. It is not only recovering the valuable metals but also protecting the environment in case they make pollution.

Primary components of the EAF dust generated during stainless steelmaking are Fe, Ni and Cr with lower concentrations of Si, Ca, Cu, Mn, Na, Mg, Pb and Zn. The chemical compositions of the EAF dust used in the present study is listed in Table 1. The X-ray diffraction patterns showed chromium mostly presents as CrO and iron as Fe_2O_3 (Fig.1). All the main phases of the dust are listed in Table 2 together with their corresponding concentrations. The metal oxides, which is important to the reduction from the industrial point of view, are CrO, Fe_2O_3/Fe_3O_4, NiO, PbO and ZnO. Several kinetics models were suggested for various solid state reductions with different forms of the non-isothermal reduction kinetics function $g(R)$[9,10]. The most suitable Eqns. considered are:

$$g(R) = 1 - (1 - R)^{1/3} = kt \quad (1)$$

$$g(R) = 1 - 2R/3(1 - R)^{2/3} = kt \quad (2)$$

$$g(R) = \ln(1 - R) = kt \quad (3)$$

They can yield the following four Eqn.s which

Table 1 Chemical compositions of EAF dust

Al	C	Ca	Cr	Fe	K	Mg	Mn
0.81	1.99	3.85	9.6	33.9	0.46	1.6	3.3
Na	Ni	P	Pb	Si	Ti	Zn	Cu
1.75	3.01	0.11	0.24	4.05	0.21	1.67	0.19

Table 2 Main phase compositions of EAF dust

Al_2O_3	CaO	CrO	Fe_2O_3	K_2O	MgO	MnO_2	Na_2O
7.08	5.39	12.55	48.41	0.55	2.65	5.22	2.36
NiO	P_2O_5	PbO	SiO_2	TiO_2	ZnO	CuO	
3.83	0.25	0.26	8.66	0.35	2.08	0.24	

① [Received date] 1999 - 09 - 18; [Accepted date] 1999 - 11 - 22

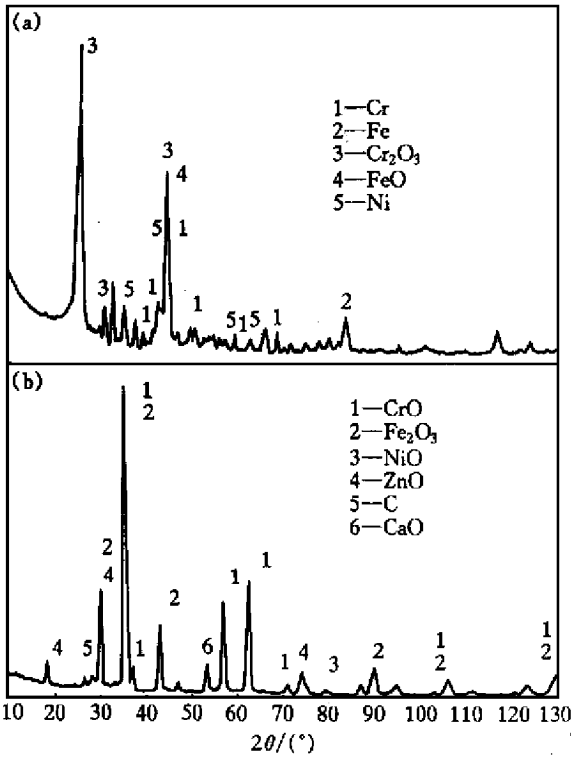

Fig.1 EAF dust XRD patterns

can be used for analysis of non-isothermal kinetics data:

$$\ln g(R)/T = \text{constant} - E/RT \quad [9] \tag{4}$$

$$\ln[g(R)/T^2] = \text{constant} - E/RT \quad [10] \tag{5}$$

$$\ln g(R) = \text{constant} - E/RT \quad [10] \tag{6}$$

$$\ln[g'(R)\,dR/dt] = \text{constant} - E/RT \quad [9,10] \tag{7}$$

After preliminarily trying to set up EAF reduction process model, it was found out that Eqn.(7) most accurately describes the EAF dust reduction process and therefore it was used in the modeling.

2 EXPERIMENTAL

2.1 Properties of EAF dust pellets

The pellets were made by mixing EAF dust with carbon, which acted as a reducing agent, and dolomite, which was used as a binder. The EAF dust was screened using a 35 mesh screen, 87% of the carbon particles were finer than 400 μm and the dolomite was crushed in a ball miller for 20 min (35 mesh screen). Four types of pellets containing 5%, 10%, 15% and 35% of carbon were studied. In each case the dolomite content was 5%. Each pellet was formed individually by progressively adding water to 1.0 g of dust, carbon, dolomite mixture and rolling it in a ceramic bowl (average diameter of the pellet was 15 mm). Different particles in the cross-section were identified by energy-dispersive X-ray spectrometer. Measurements were conducted at 20 keV accelerating voltage and 100 mA beam current. Since the carbon particles are very fine, they act as a matrix for the dust and dolomite particles. Each dust particle seems to be surrounded by carbon so that the area of contact between dust and carbon is relatively high.

2.2 Setup and apparatus

A flow chart of the experimental system used in this work is shown in Fig.2. It is a thermogravimetric analysis (TGA)/furnace, Cahn TG-171, which was connected to a temperature and heating rate control system and to a data acquisition system DAS, surrounding a cylindrical heating chamber. The temperature is measured using a B-type microthermocouple. The mass of the sample is continuously monitored by a microbalance with a 1.0 μg sensitivity. All the temperature and mass information of the sample is retrieved by the DAS and made available for analysis and visualization by the computer software. The TGA reactor includes an inlet and outlet to three reaction gases. The reactor can reach 1 700 ℃ at atmospheric pressure. The heating rate allowed is between 1.0 ℃/min and 100 ℃/min. The maximum sample mass capacity of the TGA is 100 g.

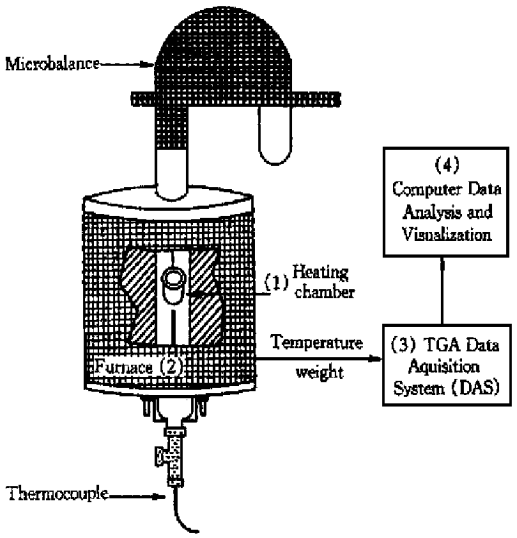

Fig.2 Schematic of thermogravimetric furnace

In the center of the heating chamber, a ceramic crucible was placed to hold the dust pellet. The temperature inside the reactor was measured by the microthermocouple located 1.0 cm below the sample crucible, which responded quickly to the changes of the conditions within the furnace (e.g. drying, volatilization and pyrolysis of the sample). Selected experiments were conducted with another microthermocouple located within the sample crucible. The temperature difference between both thermocouples was 8 ~ 14 ℃. Since the difference was relatively small (5% ~ 10% of the maximum temperature) and due to convenience, only one microthermocouple located below the sample crucible was used in most experiments. The length of the heated zone was 400

mm with a homogeneous temperature zone of 100 mm (in this zone the radial temperature profiles along the cross-section of the heating chamber are uniform). Both the crucible with the pellet sample and the microthermocouple were located within the homogeneous temperature zone.

The furnace, crucible and samples were tested separately before data acquisition experiments in order to verify the presence of mass transfer limitations and to establish the configuration appropriate for minimizing the influence of the external and internal mass transfer limitations. It was found that the external limitations were minor in comparison with the internal restrictions. Anyway the internal mass transfer limitations within the pellet were always present during the steelmaking process, therefore no precautions were necessary to reduce them. Since determination of intrinsic dust reactivity was not the purpose of this study, it was not necessary to assure that internal mass transfer effects are negligible. The average heating rate of 40 ℃/min and the nitrogen flow rate of 120 L/min, which were used in the experiments, were optimal for minimizing both the internal and external mass transfer limitations.

2.3 Procedure

In all the experiments, an average heating rate of 40 ℃/min, holding time of 30 min at the maximum temperature (1 500 ℃, which is a typical operating temperature in metallurgical operations) and subsequent cooling at a rate of 10 ℃/min were used. It was demonstrated earlier that at such condition it is possible to achieve the solid structure, in which toxic metals are encapsulated and immobilized within the dust particle, which is important from the environmental point of view. Also, the 30 min holding time at the maximum temperature assured chemical equilibrium. The additional reason for applying the average heating rate of 40 ℃/min was to simulate the ratio of the heating time scale (inverse of heating rate) to the diffusion time scale (proportional to particle radius). It is true that in industrial electric arc furnaces, the heating rate is approximately three- or four orders of magnitude higher than that applied in the TGA experiments. However, the size of the initial EAF dust particle is usually between 0.1 and 10 μm. By having a slower heating rate for a larger EAF dust pellet used in this study (15 mm), the heating/diffusion time scale ratios were comparable. The heating rate, the influence of the crucible location, sample conditions and gas flow through the TGA furnace on the measurements, were carefully verified in separate experiments. As mentioned above, the temperature in the heating chamber was measured with a microthermocouple, thus the reported heating rate was determined on the basis of the true temperature history rather than simply from the TGA-programmed temperature.

3 TREATMENT OF EXPERIMENTAL DATA

The reduction process of the EAF dust is more complex than that of a pure metal oxide. There are several metal oxides in the dust (Table 2), which are reduced simultaneously. The oxides and reduced metals formed at different stages may affect the entire reduction process. For example, the evaporation of zinc and lead must be considered in order to calculate a degree of reduction correctly. Typically, the gasification temperature of zinc is 906 ℃ and lead 1 525 ℃ after being reduced from the oxides. This will affect the calculation of the reduction degree based on the mass loss. The rate of metal evaporation can be expressed as $dm/dt = p_i(M/2\pi RT)^{1/2}$, where m is the mass of evaporated metal, t is time, p_i is a partial pressure of the evaporated metal ($\ln p_i = A/T + B$[11]; A and B are constants), M is the molecular weight of the metal, R is the gas constant and T is temperature. Therefore, the amount of evaporated metal can be calculated as follows:

$$dm = p_i(M/2\pi RT)^{1/2}dt;$$

$$dm = \int (M/2\pi RT)^{1/2}\exp[A/(T+B)]dt;$$

$$dm = \int \exp[A/(Kt+T_0)+B]\cdot [M/2\pi R(Kt+T_0)]^{1/2}dt;$$

K = heating rate,

T_0 = 1 000 K (initial temperature).

$$m = (1/K)\int (M/2\pi Rx)^{1/2}\exp(A/x+B)dx$$

$$= (2/K)(M/2\pi R)^{1/2}\int \exp[A/(y^* y)+B)]dy$$

$$= (2/K)(M/2\pi R)^{1/2}\int [1+(Ay^{-2}+B)+(Ay^{-2}+B)^2/2!+\cdots+(Ay^{-2}+B)^n/n!+\cdots]dy$$

$x = Kt + T_0$ $x = 1\,000$ when $t = 0$

$y = x^{1/2}$

At the high temperature, $(Ay^{-2}+B)n/n!$ is very small. Therefore, one can consider the main terms of the series only neglecting the latter ones, yielding the following Eqn.:

$$m = (2/K)(M/2\pi R)^{1/2}[(1+B+B^2/2)y - A(1+B)y^{-1} - A^2y^{-3}/6] + \text{constant} \quad (8)$$

Assuming that $A = -2592$ and $B = 2.19$ in the zinc evaporation process[12], the amount of evaporated zinc can be calculated as follows:

$$m_{Zn} = 2/40[65.37/(2\cdot 3.14\cdot 0.082)]^{1/2}\cdot [(1+2.19+2.19^2/2)(Kt+1\,000)^{1/2} - 2592(1+2.19)(Kt+1\,000)^{-1/2} - 2592^2(Kt+1\,000)^{-3/2}/$$

$$6] + 90.9121 \quad (9)$$

The evaporation rate of lead depends on its reduction rate suggesting that the reduction is the controlling step of the evaporation process[12]. The mass loss of lead due to evaporation in the non-isothermal reduction process can be calculated in a way similar to that for zinc, i.e. using Eqn.(9). Furthermore, it is possible to adjust the calculation of the reduction degree in order to obtain the true data, which can be used in the kinetics equation related to the reduction process, so that the mass loss of a pellet is represented by

$$\Delta m_{\Sigma} = \Delta m_{o} + \Delta m_{c} + \Delta m_{v} \quad (10)$$

where Δm_{Σ} represents total mass loss; Δm_{o} corresponds to mass loss of oxygen in metal oxides; Δm_{c} represents the mass loss of carbon and Δm_{v} represents mass loss of dust at high temperature. Thus, the degree of reduction can be determined as

$$R_t = (m_o - m_t)_{Zn} + m_{Pb}/\Delta m_{\Sigma} \quad (11)$$

where m_o represents the initial mass of the pellet; m_t is the pellet mass at time t; m_{Zn} is the mass loss due to zinc evaporation and m_{Pb} is an average mass loss due to lead evaporation.

4 RESULTS

Mass loss fraction and temperature profiles obtained during non-isothermal TGA experiments are illustrated in Fig.3. It shows that the mass loss process strongly depends on the initial amount of carbon in the EAF pellet. It is clear that low-temperature volatiles (e.g. light hydrocarbons) and moisture were nearly completely released in the early stages of the heating process. According to the chemical equilibrium calculations, reducing all metals in 100 g EAF dust requires 15.64 g of carbon, therefore, there was not enough carbon in pellets containing 5 % and 10 % C to reduce all valuable metals. In order to do it, at least 12.6 % carbon content in the pellet is needed, which is visible in the Fig.3. The profiles obtained for pellets with 5 % and 10 % carbon indicate that the reduction processes ceased early because not enough reducing agent was available. On the other hand, 35 % carbon in the pellet was much more than the required amount, therefore, the mass loss attained was lower than that for the pellet containing 15 % carbon (Fig.3), it was due to the fact that some residual carbon was present in the pellet after the reduction.

Fig.4 shows the change in the reduction degree at the function of time-temperature history. The results suggest that the initial amount of carbon in the EAF pellet does not influence the reduction mechanism up to the point, defined by temperature and time, when the reducing agent is depleted. However, the final reduction degree depends strongly on the carbon content in the pellet. The reduction degrees obtained for the pellets containing 5 %, 10 % and 15 % carbon were 53 %, 64 % and 81 %, respectively. Only in the case of the pellet with 35 % carbon, the reduction degree was 100 %. It is clear that the metal reduction process favors high concentrations of carbon. In order to compare the extents of the process, a differential rate change of the reduction degree was calculated and shown together with temperature profile as a function of time (Fig.5). The reduction process begins at 300 ℃ and the main reduction reactions take place after the temperature reaches 760 ℃. At the beginning of the process, there is a local minimum visible for the pellet containing 5 % carbon. It is due to carbon-lean conditions present in the pellet. As a result, there is no sufficient contact between dust

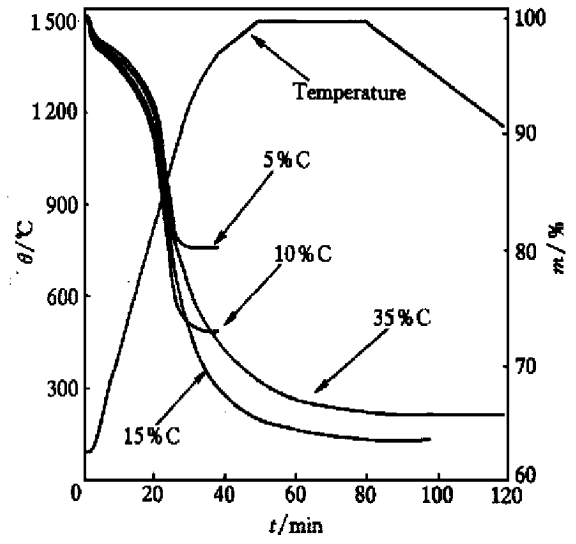

Fig.3 Profiles of mass loss fraction in TGA run

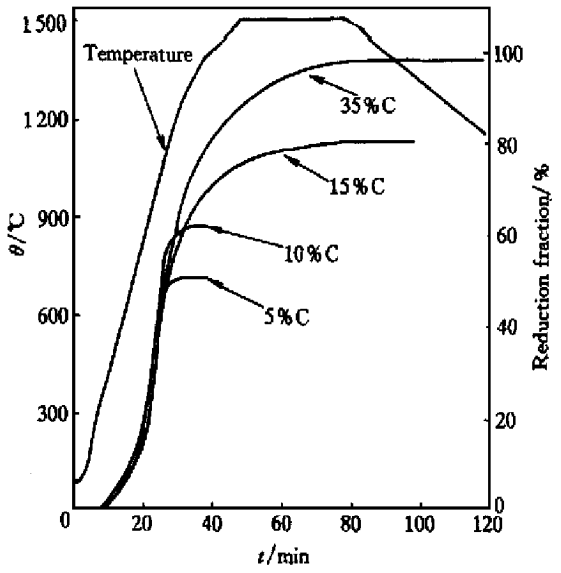

Fig.4 Profiles of reduction degree in non-isothermal TGA run

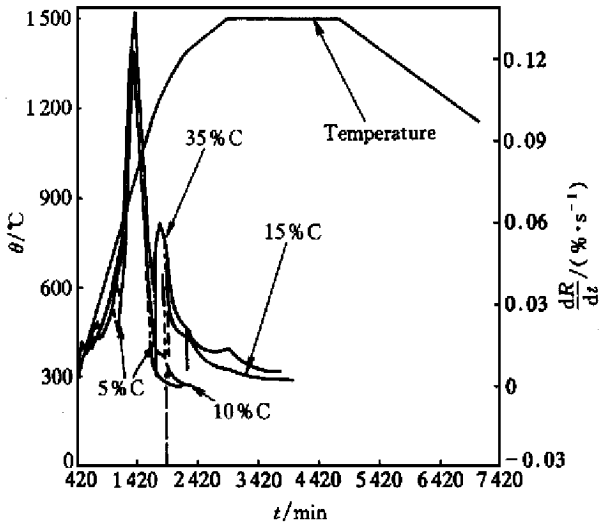

Fig.5 Profiles of reduction percentage differetiation

and carbon at their interfaces. The largest reduction rate peak for all pellets is present at 980 ℃ (approximately 1 410 s into the process) but the highest peak is attributed only to the pellet containing 35 % carbon. It may suggest that some metals, for which the reduction process is rather difficult, such as chromium, require more carbon to complete the reactions.

5 NON-ISOTHERMAL REDUCTION KINETICS

The kinetics equations have the form $g(R) = kt$. Therefore, they can be expressed as $g'(R)\,dR/dt = A(1 + htE/RT^2)\exp(-E/RT)$, where $g'(R)$ is the result of differentiation of $g(R)$ and h is the heating rate constant (can be obtained from TGA runs). htE/RT^2 is significantly lower than 1.0, thus, it could be neglected. Consequently, the above equation could be considered as $g'(R)\,dR/dt = Ae^{-E/RT}$. Therefore, $\ln[g'(R)\,dR/dt] = \text{constant} - E/RT$. Using 10 000/T as the horizontal axis and $\ln[g'(R)\,dR/dt]$ as the vertical axis it can be plotted a diagram helpful in identifying different steps of the reduction process, as well as selected kinetics parameters. The results are shown in Figs.6, 7 and 8. They identify three distinct steps of the EAF pellet reduction process in the TGA furnace. (These steps could be expected from analyzing Fig.5 where every change in the reduction rate indicates that a new mechanism dominates the current step in the reduction process).

The first step of the reduction process corre-

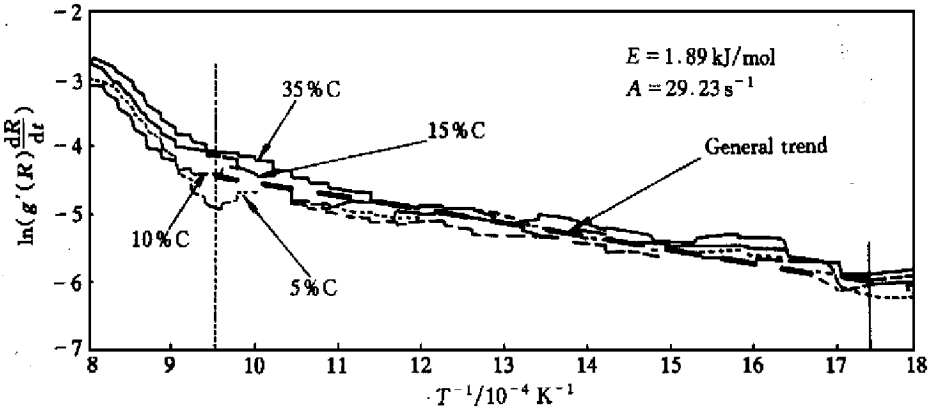

Fig.6 Evaluation of kinetic parameters in first step

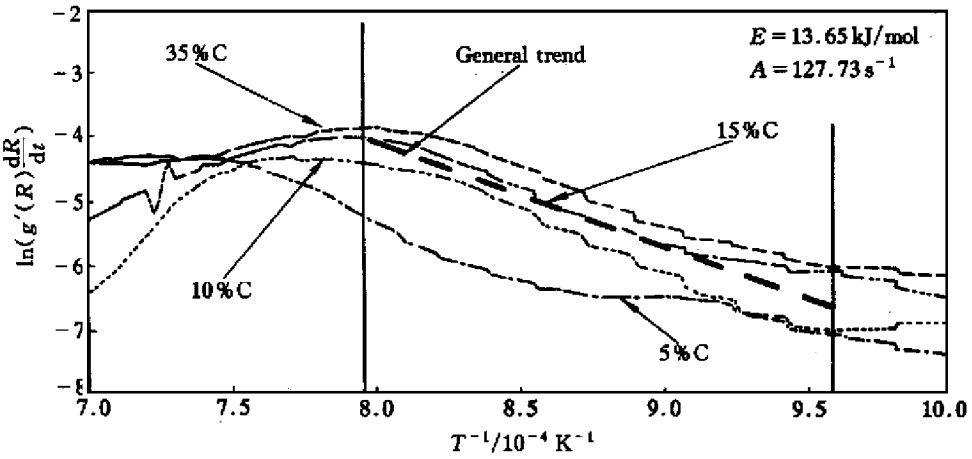

Fig.7 Evaluation of kinetic parameters in second step

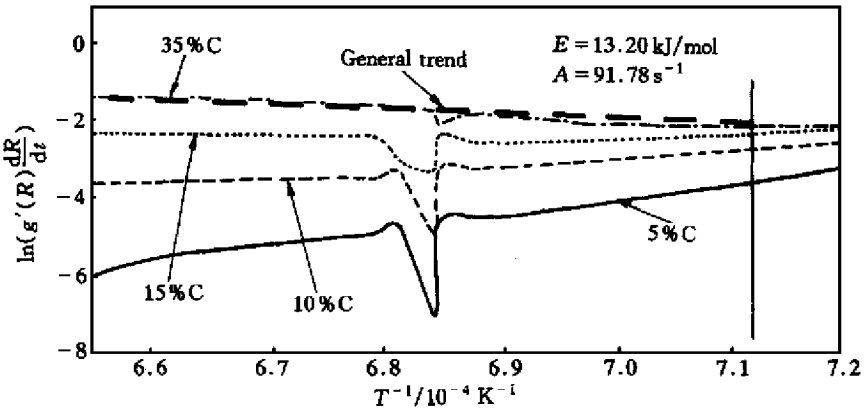

Fig.8 Evaluation of kinetic parameters in third step

sponds to the temperature range from 300 ℃ to 760 ℃ and the time range from 7 min to 18 min (Fig. 6 and Fig.5). In this step the following reactions are dominated:

$$Fe_mO_n + C = Fe_mO_{n-1} + CO$$

and

$$NiO + C = Ni + CO$$

because there was no oxygen available in the furnace and only these two reactions could process at low temperatures. These reactions were taken place in the regions of the EAF pellet where carbon and metal oxides were contact with each other in direct. Such reduction process conforms to the first order rules and the process is controlled by the chemical reaction. It could be represented by the following kinetic Eqn.:

$$1 - (1 - R)^{1/3} = kt \quad (12)$$

where $k = A\exp(-E/RT)$, apparent activation energy $E = 108.9$ kJ/mol, frequency factor $A = 29.23\ s^{-1}$. The kinetics parameters E and A were calculated using data available from Fig.7. In this Fig. the four curves representing different carbon content in pellet are almost parallel and located relatively close to one another. A dashed line showing the general trend of the curves can interpolate them. The slope of the dashed line was used to calculate the apparent activation energy and frequency factor. The apparent activation energy $E = 83.14$ kJ/mol and the intercept of the line at $10000/T = 0$ is the frequency factor A. The apparent activation energy is very low for this step, it means that the reactions can easily take place and proceed. There is no iron formed in this step since it requires significantly higher reduction temperature according to surface thermodynamics[13]. On the other hand, the reduction constant k equals to constant/ρr_0, where ρ is the density of the reactant and r_0 is the initial radius of the dust particles. The reaction rate will increase in this step when the density and size of the dust are small. The second step of the reduction process corresponds to a higher temperature range from 760 ℃ to 980 ℃ (Fig.7 and Fig. 5). In this step the reduction process is most extensive with the majority of iron oxides being reduced. The migration of both carbon and metal oxides in the reduced solid phase is becoming so difficult that carbon monoxide CO fulfills the role of the reducing agent rather than carbon. The following reactions will occur:

$$Fe_mO_n + CO = Fe_mO_{n-1} + CO_2$$

$$NiO + CO = Ni + CO_2$$

$$ZnO + CO = Zn + CO_2$$

$$PbO + CO = Pb + CO_2$$

$$C + CO_2 = 2CO$$

Consequently, the following sequence of processes is expected and illustrated by a shrinking core model:

1) CO transfers from the pellet's interior to the surface of Me (reduced metal);

2) CO transfers through the Me to the surface of MeO (metal oxides);

3) CO is absorbed at the surface of the MeO;

4) CO reacts with MeO to form the products Me and CO_2;

5) CO_2 is desorbed from the surface of MeO;

6) CO_2 transfers through the Me to the pellet;

7) CO_2 reacts with carbon to form CO.

Thus, the reduction process in the second step is controlled by the diffusion of gases in the reduced metal and can be represented by the following kinetics Eqn.:

$$1 - 2R/3 - (1 - R)^{2/3} = kt \quad (13)$$

where $k = A\exp(-E/RT)$, apparent activation energy $E = 130.65$ kJ/mol, frequency factor $A = 127.73\ s^{-1}$. These kinetics parameters are obtained via calculations based on data shown in Fig.7. The kinetics constant $k = \text{constant} \cdot MD\Delta c/(\alpha r_0)$, where M represents the molecular weight of the reactant; $D = D_0\exp(-E/RT)$ is Fick's diffusion constant; Δc is the CO concentration difference between the oxides surface and the pellet interior; α is the stoichiometric ratio of the reactants (in reaction nMeO + mCO = products, $\alpha = m/n$); ρ and r_0 are the same as in the first step. The reaction rate can be increased in this step by increasing the temperature and porosity of re-

duced metals and by decreasing density and size of the dust.

The last step of the reduction process begins at 980 ℃ (Fig.8). Initially, up to 1170 ℃, influence of the carbon concentration in the pellets on the reduction process is not observed (Fig.5). However, when the temperature increases over 1170 ℃, the reduction process seems to depend on the residual carbon in the pellet. Only the pellet with the initial carbon content of 35 % is able to support continuous reduction. The reduction of CrO may begin only at 1170 ℃. Thus, the CrO reduction process could proceed if the following two conditions were fulfilled:

1) sufficiently high temperature (>1170 ℃);

2) high initial (and residual) carbon concentration. The kinetics Eqn. relevant to stage 3 could be expressed as:

$$dR/dt = k(1 - R) \quad (14)$$

or

$$\ln(1 - R) = -kt \quad (15)$$

where $k = A\exp(-E/RT)$, apparent activation energy $E = 130.2$ kJ/mol, frequency factor $A = 91.78\ s^{-1}$. The kinetics parameters were obtained from Fig.8 in the same manner as for stages 1 and 2.

6 ANALYSES OF REDUCTION PROCESS AND KINETICS PARAMETERS

The apparent activation energies calculated in this work are smaller, especially in the second step when iron oxides are reduced, than those obtained by other researchers on the kinetics of iron ore reduction[9,10,14~17]. It is due to distinctly different composition of the EAF pellets as compared with iron ore. In addition, data presented in this paper concern non-isothermal conditions (almost exclusively isothermal experiments were previously conducted to determine reduction characteristics). It indicates that the presence of additional metal oxides in the pellet diminishes the activation energy stimulating the reduction process. It should also be mentioned that the apparent activation energy measured under non-isothermal temperature condition is much smaller than that under the isothermal condition.

The kinetics Eqns. could not precisely describe the CrO reduction. This process takes place in the last step of reduction and only the pellets with 35 % initial carbon content reveals its presence. The reduction kinetics of CrO could be expressed by $g(R) = -\ln(1 - R) = kt$. This formula has also been proposed by Ray et al[18] who also absolved CrO reduction at the end of the entire process.

[REFERENCES]

[1] LI Ding-yi. Application of plasma technology to treat EAF dust [J]. Iron and Steel, 1995, 30(3): 72 - 74.

[2] Jensen J T. Reduction of EAF dust emissions by injecting it into the furnace [J]. Metallurgical Plant and Technology International, 1997(6): 58 - 62.

[3] Schoukens A F S. The enviroplas process for the recovery of zinc, chromium and nickel from steel-plant dust [A]. USA, Electric Furnace Conference Proceedings [C], 1996. 341 - 350.

[4] John Floyd. EAF dust treatment in an Ausmelt furnace system [J]. SEAISI Quarterly, 1993(4): 60 - 65.

[5] Mastsuoka S. New technology for treating electric arc furnace dust [J]. Iron & Steel Engineer, 1991(2): 37 - 40.

[6] Evans L G. Recycling of EAF dust by direct injection [A]. USA, ISS, Electric Furnace Conference Proceedings [C], 1986.

[7] Charles J Labee. Update on electric arc furnace dust treatment [J]. Iron and steel Engineer, 1992(5): 48 - 49.

[8] Neil. EAF Dust Characteristics and Behavior during Thermal Treatment [D]. Department of Metallurgical Engineering of McGill University, 1998.

[9] Paul S and Mukherjee S. Non-isothermal and isothermal reduction kinetics of iron ore agglomerates [J]. Ironmaking and Steelmaking, 1992, 19(3): 190 - 193.

[10] Prakash S. Non-isothermal kinetics of iron ore reduction [J]. Ironmaking and Steelmaking, 1994, 21(3): 237 - 243.

[11] WEI Shou-kun. Thermodynamics of Metallurgical Process [M]. Shanghai: Shanghai Science and Technology Press, 1980. 344 - 352.

[12] QU Ying. Principle of Steelmaking [M]. Beijing: Metallurgical Industry Press, 1980. 73 - 74.

[13] Dancy T E. The development of direct reduction processes [J]. Scandinavian Journal of Metallurgy, 1993 (22): 100 - 108.

[14] Mazumder A K, Sharema T and Reddy G V. Reduction kinetics of iron oxide pellet by non-coking coal [J]. Transactions of the Indian Institute of Metals, 1989, 42 (3): 299 - 305.

[15] Mourao M B and Capocchi J D T. Rate of reduction of iron oxide in carbon-bearing pellets [J]. Trans Instn Min Metall, 1996, 105: 9 - 12.

[16] Basu P, Sarkar S B and Ray H S. Isothermal reduction of coal mixed iron oxide pellets [J]. Transactions of the Indian Institute of Metals, 1989, 42(2): 165 - 172.

[17] Ding Y L and Warner N A. Kinetics and mechanism of reduction of carbon-chromite composite pellets [J]. Ironmaking and Steelmaking, 1997, 24(3): 224 - 230.

[18] Ray H S, Sarangi B and Sarangi A. Kinetics of aluminothermic reduction of Cr_2O_3 thermoanalytical investigation [J]. Scandinavian Journal of Metallurgy, 1996, 25(6): 256 - 264.

(Edited by HUANG Jin-song)